

# Single Electron Detection and Spectroscopy

Savanna Rae Starko

Washington and Jefferson College, Washington, Pennsylvania 15301

(Dated: 29 August 2015)

This paper describes the development of a distribution of average magnetic fields experienced by trapped electrons as it relates to the creation of decay electron energy spectra from measurements of their cyclotron frequencies. Two trapping magnetic field configurations are explored, being a truncated harmonic and a magnetic bottle, and the change in trapping efficiency with variations in trap dimensions is considered for the magnetic bottle. Determining the likely average magnetic field with which a trapped electron interacts is beneficial in understanding the process of nuclear beta decay and in exploring questions about nuclear beta decay that could lead to new physics.

## I. INTRODUCTION

Project 8, a neutrino mass experiment at the University of Washington, aims to infer the mass of the neutrino from the shape of the energy spectrum for decay electrons from tritium beta decay. Project 8 is known for having made the first measurement of single-electron cyclotron radiation with the experimental set-up pictured in Figure I.1[2].

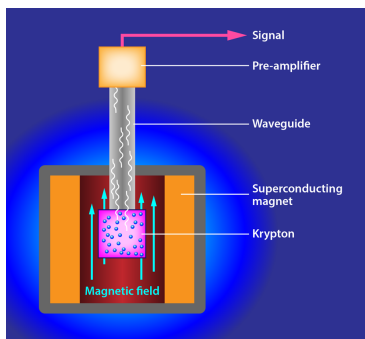


FIG. I.1. Project 8 Set-up

The apparatus includes a small volume of gas contained in what is known as the cell[1]. This gas is krypton, a byproduct of the decay of rubidium. As byproducts of this decay as well, electrons within the cell are affected by the presence of a magnetic field. A superconducting magnet provides a main field of approximately 1-T directed along the vertical[1]. A small copper coil introduces an inhomogeneous magnetic field within the cell. This inhomogeneity in the field ( $\vec{B}$ ) causes a fraction of the electrons to feel a force directed toward the center of the cell according to

$$\vec{F} = \vec{\nabla} (\vec{\mu} \cdot \vec{B}), \quad (\text{I.1})$$

where  $\vec{\mu}$  is the electron's orbital magnetic moment. The electrons subjected to this force are trapped. The cyclotron frequency ( $f_\gamma$ ) for each of these trapped electrons is determined by the following for-

mula:

$$f_\gamma = \frac{eB}{2\pi\gamma m}, \quad (\text{I.2})$$

where  $e$  is the electron charge,  $B$  the magnetic field directed perpendicularly to the electron's cyclotron orbit,  $m$  the electron mass, and  $\gamma$  the Lorentz factor. The Lorentz factor ( $\gamma$ ) is a function of the electron's kinetic energy, with formula:

$$\gamma = \left(1 + \frac{K}{mc^2}\right), \quad (\text{I.3})$$

where  $K$  is the electron's kinetic energy and  $m$  its mass. The electrons trapped within the cell will radiate power and lose kinetic energy over time. Signals from this power radiation travel along a 1-m length of waveguide to receivers and digitizers for analysis. Analysis of these signals leads to the creation of frequency spectra for single-electron events.

Equation I.3 indicates that the value of  $\gamma$  for an electron losing kinetic energy will decrease. When  $\gamma$  decreases, Equation I.2 indicates that the cyclotron frequency of the electron increases. Thus, the frequency spectrum for a single electron will indicate a linear relationship between frequency and time. From each frequency spectrum for a single electron can be extracted its approximate initial emission frequency. The initial emission frequencies for many electrons are used to create an energy spectrum for the decay electrons in total with the relationship between frequency and kinetic energy given by Equation I.2 in mind. The goal of Project 8 maintains that the shape of this spectrum will elucidate the mass of the neutrino.

## II. MOTIVATION

According to the formula given by Equation I.2, the cyclotron frequency for a given electron is a function of both its kinetic energy and the magnetic field with which it interacts. Given the random nature of decay, a trapped electron may originate with any initial position within the dimensions of the trap; the initial angle of its momentum vector with respect

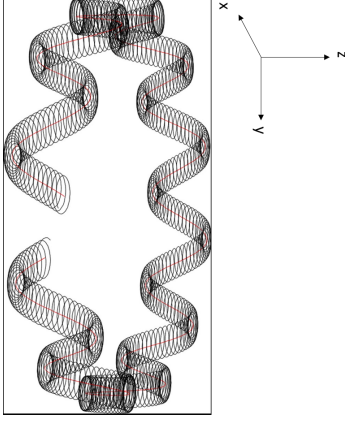


FIG. I.2. Three Oscillation Types

to the magnetic field can assume any value within a range of trapping angles based on its initial position. There are three oscillation types pertinent to the trapped electron as shown in Figure I.2: cyclotron oscillation,  $z$ -oscillation, and magnetron oscillation. Cyclotron frequencies are on the order of 20 GHz.  $Z$ -oscillation is on the order of MHz, and frequency of the magnetron motion follows on the order of kHz. Thus, there lies difficulty in determining precisely the magnetic field with which a trapped electron interacts. However, it is possible to calculate a distribution of the average magnetic fields ( $\bar{B}$ ) for trapped electrons, which is one task of this research project.

With this distribution, the average magnetic field that an electron is likely to experience can be determined and incorporated into energy calculations. Solving Equation I.2 for  $\gamma$  gives

$$\gamma = \frac{eB}{2\pi f_\gamma m}. \quad (\text{II.1})$$

Equation II.1 shows that with the initial emission frequency measurement ( $f_\gamma$ ) as found according to the methods described in Section I for a given electron and the average value of the average magnetic field ( $\bar{B}$ ) experienced by that electron, the electron's  $\gamma$  is obtainable. Then, solving Equation I.3 gives the following

$$K = (\gamma - 1) mc^2 \quad (\text{II.2})$$

for the electron's kinetic energy ( $K$ ). Utilizing methods of calculating electron energies such as this one makes evident the possibility of discovering new physics in relation to nuclear decay.

### III. METHODS OF CALCULATION

A magnetic bottle is the magnetic field configuration applicable to Project 8. This field configuration re-

sults from an arrangement of two coils running current in the same direction; the field is stronger at the ends of this configuration than at the center. The following section uses first a simpler model for a field configuration to display many of the properties behind electron trapping.

#### A. On-Axis Calculation

The first type of magnetic field configuration examined is that of a truncated quadratic trap, pictured below:

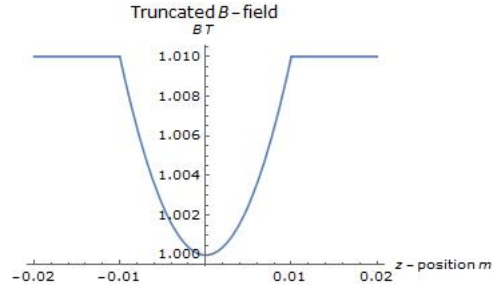


FIG. III.1. Truncated Quadratic Field

The field equation corresponding to a trap of this type is as follows:

$$\vec{B} = B_0 \left( 1 + \frac{z^2}{L^2} \right) \hat{z}, \quad (\text{III.1})$$

where  $z$  is the position at which a decay electron originates along the  $z$ -axis,  $B_0$  is the main magnetic field of 1-T, and  $L$  is a parameter used to control the depth of the trap. For this first calculation,  $L$  is set at 10-cm. The maximum extent of the magnetic field is set at 1.01-T, and the maximum  $z$ -extent of the trap is set at 1.0-cm.

The electrons trapped in this field configuration each possess a magnetic moment that can be determined classically. Approximating the electron's motion as that of a loop of circulating current in a magnetic field directed along  $z$ , its magnetic moment  $\vec{\mu}$  is

$$\vec{\mu} = \frac{-evR}{2} \hat{z},$$

where  $e$  is the electron charge,  $v$  the electron's tangential velocity along its cyclotron orbit, and  $R$  the radius of that orbit. The magnetic moment can be rewritten in terms of the kinetic energy in the transverse direction ( $E_\perp$ ). This, along with the idea that the radius of the cyclotron orbit  $R = \frac{\gamma mv}{eB}$  for mass  $m$  and charge  $e$ , gives the following:

$$\vec{\mu} = \frac{-E_\perp}{B} \hat{z}.$$

This equation for the magnetic moment can be utilized to determine the force an electron experiences

due to inhomogeneity in the magnetic field and the consequential equation of motion for the electron.

### 1. Force and Equation of Motion Along $z$

The electron is subjected to a force ( $\vec{F}$ ) based on its magnetic moment  $\vec{\mu}$  and the magnetic field given by Equation III.1 according to what follows:

$$\begin{aligned} F_z &= \nabla_z (\vec{\mu} \cdot \vec{B}) \\ &= \frac{-E_\perp}{B} B_0 \left( \frac{2z}{L^2} \right) \hat{z}. \end{aligned} \quad (\text{III.2})$$

From this force and according to Newton's second law, we establish that the angular frequency of oscillation  $\omega = \sqrt{\left(\frac{E_\perp}{mB}\right) B_0 \left(\frac{2}{L^2}\right)}$ . Since the force on the trapped electron is proportional to its initial position ( $z$ ), we also give, based on Newton's second law, the equation of position the form:

$$\vec{z} = z_{\max} \sin \omega t \hat{z}. \quad (\text{III.3})$$

In this functional form,  $z_{\max}$  is the maximum  $z$ -position attainable by a trapped electron with initial position  $z$  and initial angle  $\phi$  between its momentum vector and the magnetic field.

### 2. Finding $z_{\max}$ and Time-averaged Magnetic Field ( $\bar{B}$ )

An important invariant to this series of calculations is the magnetic moment  $\vec{\mu}$ . Since  $\vec{\mu}$  is conserved, the following relationship holds and lends itself to solving for the trapped electron's maximum  $z$ -position,  $z_{\max}$ . When the electron's momentum vector is at angle  $\phi_{\max} = 90^\circ$ , the electron stops moving along  $z$  and has therefore reached its maximum  $z$ -position. The following array of equations depicts this scenario:

$$\begin{aligned} \frac{\sin^2 \phi}{\sin^2 \phi_{\max}} &= \frac{B(z)}{B(z_{\max})} \\ \sin^2 \phi &= \frac{B_0 \left(1 + \frac{z^2}{L^2}\right)}{B_0 \left(1 + \frac{z_{\max}^2}{L^2}\right)} \\ z_{\max} &= \sqrt{\csc^2 \phi (L^2 + z^2) - L^2}. \end{aligned} \quad (\text{III.4})$$

The value of the time-averaged magnetic field ( $\bar{B}$ ) will depend on the  $z$ -motion of the particle, described by Equation III.3 and with functional form for  $z_{\max}$  given by Equation III.4. With these considerations and by averaging the field Equation III.1 over a period of the electron's oscillation ( $T$ ), the resulting  $\bar{B}$  is given by

$$\begin{aligned} \bar{B} &= \frac{1}{T} \int_0^T B_0 \left(1 + \frac{z_{\max}^2 \sin^2 \omega t}{L^2}\right) dt \hat{z} \\ &= B_0 \left[1 + \frac{z_{\max}^2}{2L^2}\right] \hat{z}. \end{aligned} \quad (\text{III.5})$$

This functional form for  $\bar{B}$  indicates that the average magnetic field experienced by a trapped electron is a function of its initial position  $z$ , the initial  $\phi$  between its momentum vector and the magnetic field, the main magnetic field  $B_0$ , and the parameter  $L$ .

### 3. Range of Trapped Angles

In order to create a distribution of the average magnetic fields  $\bar{B}$  experienced by trapped electrons, it is essential to consider the range of pitch angles  $\phi$  with respect to  $z$  that an electron may possess to remain trapped. Considering a magnetic field directed along  $z$  and a system of Cartesian coordinates, the range of trapped angles  $\phi$  is symmetric about the  $xy$ -plane. Due to this symmetry, this calculation considers a maximum trapped angle of  $90^\circ$  with respect to  $z$ . The minimum trapped angle for an electron originating at position  $z$  along the axis is determined under the assumption that the maximum magnetic field ( $\vec{B}$ ) the electron experiences is the maximum extent of the magnetic field overall ( $B\left(\frac{\Delta z}{2}\right)$ ), where  $\frac{\Delta z}{2}$  is again equal to 1.0-cm. Utilization of the conservation of the magnetic moment gives the following:

$$\begin{aligned} \frac{\sin^2 \phi}{\sin^2 \phi_{\max}} &= \frac{B(z)}{B\left(\frac{\Delta z}{2}\right)} \\ \sin^2 \phi &= \frac{B(z)}{B\left(\frac{\Delta z}{2}\right)} \\ \phi &= \arcsin \sqrt{\frac{B(z)}{B\left(\frac{\Delta z}{2}\right)}}. \end{aligned}$$

Hence, the pertinent range of trapped angles is:

$$\arcsin \sqrt{\frac{B(z)}{B\left(\frac{\Delta z}{2}\right)}} \leq \phi \leq 90^\circ.$$

### 4. Ranges of Average Field and $z$ -position

When a trapped electron originating along  $z$  experiences its minimum trapped pitch angle  $\phi$ , it is bound to reach the maximal value for  $\bar{B}$ . This maximal  $\bar{B}$  for the electron is given by

$$\begin{aligned} \bar{B} &= B_0 \left(1 + \frac{z_{\max}^2}{2L^2}\right) \\ &= B_0 \left(1 + \frac{1}{2L^2} (\csc^2 \phi_{\min} (L^2 + z^2) - L^2)\right) \\ &= B_0 \left(1 + \frac{1}{2L^2} \left(\left(\frac{B\left(\frac{\Delta z}{2}\right)}{B(z)}\right) (L^2 + z^2) - L^2\right)\right) \\ &= \frac{B_0 + B\left(\frac{\Delta z}{2}\right)}{2} \end{aligned} \quad (\text{III.6})$$

since its motion leads it to the maximum value for  $\bar{B}$ . At a maximum initial pitch angle  $\phi$  of  $90^\circ$  with respect to  $z$ , the electron experiences a minimal value for  $\bar{B}$  based on its initial  $z$ -position. This lower limit is given by

$$\begin{aligned}\bar{B} &= B_0 \left( 1 + \frac{1}{2L^2} (\csc^2 \phi_{\max} (L^2 + z^2) - L^2) \right) \\ &= B_0 \left( 1 + \frac{1}{2L^2} ((L^2 + z^2) - L^2) \right) \\ &= \frac{B_0 + B(z)}{2}\end{aligned}\quad (\text{III.7})$$

since the electron does not explore higher values of the magnetic field than that at the position at which it originates. This lower limit on  $\bar{B}$  stipulates a range of applicable  $z$  values for an electron experiencing a given  $\bar{B}$  according to the following:

$$-L\sqrt{2\left(\frac{\bar{B}}{B_0} - 1\right)} < z < L\sqrt{2\left(\frac{\bar{B}}{B_0} - 1\right)}.\quad (\text{III.8})$$

The trapping ranges considered in Sections III.A.3–4 for  $\phi$ ,  $\bar{B}$ , and  $z$  apply in constructing the probability density function for  $\bar{B}$ .

#### 5. Constructing the Probability Density Function

The distribution of average magnetic fields  $\bar{B}$  is given by the probability density function for  $\bar{B}$ . This function is constructed according to the following relationship:

$$\frac{dN}{d\cos\phi} = \frac{dN}{d\bar{B}} \frac{d\bar{B}}{d\cos\phi},\quad (\text{III.9})$$

where  $N$  is a number of electron trapping events. The term on the left-hand side of Equation III.9 is considered constant such that some spherical volume is uniformly populated with trapping events.

What is desired on the right-hand side of the equation is the first term: how the number of trapping events changes with  $\bar{B}$ . What can be calculated is the second term on the right-hand side of the equation, based on the functional form for  $\bar{B}$  given by Equation III.5.

First, since  $d(\cos\phi) = \sin\phi d\phi$ , an expression for  $\sin\phi$  in terms of  $\bar{B}$ ,  $z$ , and constants is determined given the functional form for  $\bar{B}$ . This leads to the following:

$$\sin\phi = \frac{1}{L} \sqrt{\frac{B_0(L^2 + z^2)}{2\bar{B} - B_0}}.\quad (\text{III.10})$$

Similarly, an equation for  $d\phi$  in terms of  $\bar{B}$ ,  $z$ , and constants is determined to be the following:

$$d\phi = d\bar{B} \frac{-1}{(2\bar{B} - B_0)} \sqrt{\frac{B_0(L^2 + z^2)}{(2\bar{B} - B_0)L^2 - B_0(L^2 + z^2)}}.\quad (\text{III.11})$$

Equations III.10 and III.11 multiplied together give an equation for how the probability density changes with  $\bar{B}$  ( $\frac{dP}{d\bar{B}}$ ) in terms of  $\bar{B}$ ,  $z$ , and constants. This equation is as follows:

$$\frac{dP}{d\bar{B}} = \frac{-A(B_0)(L^2 + z^2)}{L(2\bar{B} - B_0)^{\frac{3}{2}} \sqrt{(2\bar{B} - B_0)L^2 - B_0(L^2 + z^2)}},\quad (\text{III.12})$$

where  $A$  is some normalization constant. The goal is to find the probability density for a particular value of  $\bar{B}$ . Given that Equation III.12 is in terms of  $\bar{B}$  and  $z$ , the next step of this calculation is to integrate that equation over the range of  $z$  values applicable to a given  $\bar{B}$ . This range is given by Inequality III.8. In addition, the range of  $\bar{B}$  given in Section III.A.4 must be considered. This means that the integral Equation III.12 over applicable  $z$  will evaluate for values of  $\bar{B}$  greater than the main field  $B_0$  and less than  $\frac{B_0 + B(\frac{\Delta z}{2})}{2}$ ; otherwise, the integral evaluates to 0. The desired function is given by Equation III.13, where  $f(z, \bar{B})$  is Equation III.12.

$$\begin{aligned}\frac{dN}{d\bar{B}} &= 2H(\bar{B} - B_0)H\left(\frac{B_0 + B_{\max}}{2} - \bar{B}\right) \int_0^{L\sqrt{2\left(\frac{\bar{B}}{B_0} - 1\right)}} f(z, \bar{B}) dz \\ &= H(\bar{B} - B_0)H\left(\frac{B_0 + B_{\max}}{2} - \bar{B}\right) \left(\frac{-\pi L\bar{B}}{\sqrt{B_0}(2\bar{B} - B_0)^{\frac{3}{2}}}\right).\end{aligned}\quad (\text{III.13})$$

This is the probability density function for  $\bar{B}$  given that a trapped electron originates along the  $z$ -axis with position  $z$  and angle  $\phi$  between its momentum vector and the direction of the magnetic field.

#### 6. Comparison to the Monte Carlo

In a Monte Carlo simulation, a series of similar calculations can be performed. Each of some number of electrons is randomly assigned a position  $z$  within the  $z$ -extent of the trap. In addition, each electron is randomly given an initial pitch angle  $\phi$  with respect to the magnetic field. With this information,

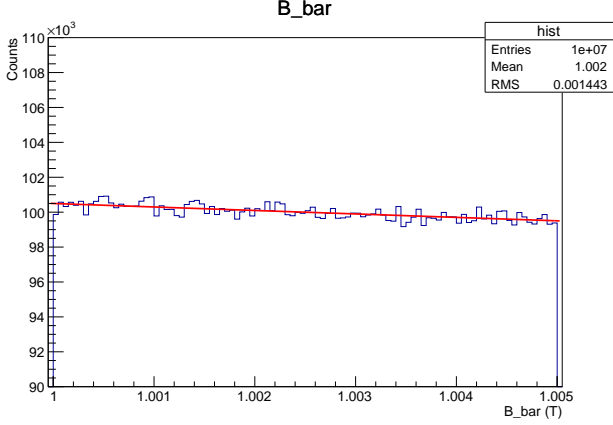


FIG. III.2. Distribution of  $\bar{B}$ -values On-axis

the simulation calculates the magnetic field experienced by each electron and determines whether it is trapped according to the range of allowable trapping angles.

If an electron is in fact trapped, the simulation will calculate the average magnetic field it experiences based on its maximum  $z$ -position. Then, a histogram of all determined  $\bar{B}$ -values is plotted. Overlaying the red analytical function in Equation III.13 with this blue histogram produces Figure III.2, showing close agreement between analytical solution and simulation.

### 7. Relating the Analytical Solution and Monte Carlo

Manipulation of Equation III.4 allows the quantity  $\left(\frac{z_{\max}}{L}\right)^2$  to be represented as follows:

$$\left(\frac{z_{\max}}{L}\right)^2 = \left(\frac{\cos^2 \phi + \left(\frac{z}{L}\right)^2}{\sin^2 \phi}\right). \quad (\text{III.14})$$

Substituting Equation III.14 into Equation III.5 gives the following:

$$\frac{\bar{B}}{B_0} = \left[1 + \frac{\cos^2 \phi + \left(\frac{z}{L}\right)^2}{2 \sin^2 \phi}\right].$$

When  $\cos \phi$  is near 0 and  $\sin \phi$  is near 1, the value of  $\frac{\bar{B}}{B_0}$  increases slowly for fixed  $z$ . As  $\cos \phi$  approaches 1 and  $\sin \phi$  goes to 0, the value of  $\frac{\bar{B}}{B_0}$  begins to increase more quickly. Figure III.3 considers the ratio of  $\frac{\bar{B}}{B_0}$  as a function of  $\cos \phi$  for a fixed  $z$ ,  $z = 0$ . For  $z = 0$ , the range of trapped angles considered is from approximately  $84.3^\circ$  to  $90^\circ$ , corresponding to a range for cosine of 0 to approximately 0.0993.

Figure III.3 shows that there is a higher concentration of events at  $\phi$ -values closest to  $90^\circ$ , and the number of events tapers-off with decreasing angle and increasing field strength. This helps to ex-

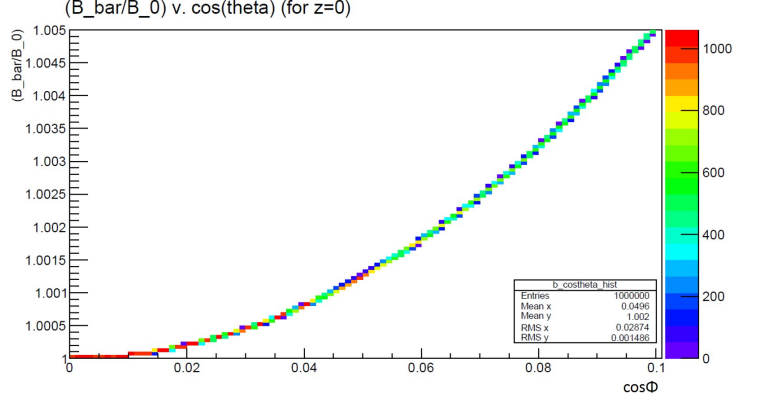


FIG. III.3.  $\frac{\bar{B}}{B_0}$  versus  $\cos \phi$  for  $z = 0$ . As  $\cos \phi$  grows, the fraction of electrons trapped decreases.

plain why Figure III.2 shows the on-axis distribution function for  $\bar{B}$  peaking near  $B_0$ .

### B. Off-Axis Calculation

The next field configuration examined for this research is that of a magnetic bottle. Now, decay electrons originate with some position ( $z$ ) along the  $z$ -axis, some radius ( $r$ ) with respect to the  $z$ -axis, and some pitch angle ( $\phi$ ) with respect to the magnetic field ( $\vec{B}$ ). The field equations corresponding to a trap of this type are as follows:

$$B_r = \frac{-B_0 r z}{L^2}$$

$$B_\theta = 0$$

$$B_z = B_0 \left(1 + \frac{z^2}{L^2}\right) - \frac{B_0 r^2}{2L^2}.$$

The  $z$ -component of this field can be represented according to Equation III.1 with an appropriate change of variables:

$$B_0 \rightarrow B'_0 = B_0 \left(1 - \frac{r^2}{2L^2}\right) \quad (\text{III.15})$$

$$L \rightarrow L' = L \sqrt{\left(1 - \frac{r^2}{2L^2}\right)} \quad (\text{III.16})$$

$$B\left(\frac{\Delta z}{2}\right) \rightarrow B'\left(\frac{\Delta z}{2}\right) = B_0 \left(1 + \frac{\left(\frac{\Delta z}{2}\right)^2}{L^2} - \frac{r^2}{2L^2}\right). \quad (\text{III.17})$$

#### 1. Finding $z_{\max}$ and Time-averaged Magnetic Field $\bar{B}$

As with the on-axis case, the idea that the magnetic moment is invariant is essential in determining the maximum  $z$ -position ( $z_{\max}$ ) for a given electron with

initial  $z$ -position ( $z$ ), initial pitch angle ( $\phi$ ), and radius of orbit ( $r$ ). Solved in the same fashion as Section III.A.2, this gives the following for  $z_{\max}$ :

$$\frac{\sin^2 \phi}{\sin^2 \phi_{\max}} = \frac{B(z)}{B(z_{\max})}$$

$$\sin^2 \phi = \frac{B_0 \left(1 + \frac{z^2}{L^2}\right) - \frac{B_0 r^2}{2L^2}}{B_0 \left(1 + \frac{z_{\max}^2}{L^2}\right) - \frac{B_0 r^2}{2L^2}}$$

$$z_{\max} = L \sqrt{((\csc^2 \phi - 1) + \frac{z^2}{L^2} \csc^2 \phi - \frac{r^2}{2L^2} (\csc^2 \phi - 1))}. \quad (\text{III.18})$$

This information about the maximum attainable  $z$ -position for a given electron applies in calculating the time-averaged magnetic field ( $\bar{B}$ ) it experiences.

---


$$\frac{dN}{d\bar{B}} = H(\bar{B} - B'_0) H\left(\frac{B'_0 + B'_{\max}}{2} - \bar{B}\right) \left(\frac{-\pi L' \bar{B}}{\sqrt{B'_0(2\bar{B} - B'_0)^{\frac{3}{2}}}}\right). \quad (\text{III.20})$$


---

This Equation III.20 is in terms of  $r$  and  $\bar{B}$ . Thus, it must be integrated over the range of  $r$  applicable to a given  $\bar{B}$ . This integral is performed in three parts according to following bounds:

$$B'_0(r_{\max}) \leq \bar{B} < B'_0(r = 0)$$

$$B'_0(r = 0) \leq \bar{B} < \bar{B}(r_{\max}, \frac{\Delta z}{2})$$

$$\bar{B}(r_{\max}, \frac{\Delta z}{2}) \leq \bar{B} \leq \bar{B}(r = 0, \frac{\Delta z}{2}).$$

The limits on  $r$  differ for each of these three subranges of  $\bar{B}$ . For the first range of  $\bar{B}$  examined,  $B'_0(r_{\max})$  is the minimum possible extent for  $\bar{B}$  overall, and  $B'_0(r = 0)$  is the minimum extent of  $\bar{B}$  at  $r = 0$ . Each of these  $\bar{B}$ -values applies at some minimum radius given by the Heaviside function  $H(\bar{B} - B'_0)$  through  $r_{\max}$ , the maximum possible radius considered. The bounds for  $r$  applicable to this range of  $\bar{B}$  are given by

$$L \sqrt{2 \left(1 - \frac{\bar{B}}{B_0}\right)} < r < r_{\max}. \quad (\text{III.21})$$

For the second range of  $\bar{B}$  examined,  $\bar{B}(r_{\max}, \frac{\Delta z}{2})$  is the maximum extent for  $\bar{B}$  at the maximum radius  $r_{\max}$  considered. All values of  $\bar{B}$  within this range are applicable at radii from  $r = 0$  through  $r = r_{\max}$ . The bounds for  $r$  applicable to this range of  $\bar{B}$  are given by

$$0 < r < r_{\max}. \quad (\text{III.22})$$

For third range of  $\bar{B}$  examined,  $\bar{B}(r = 0, \frac{\Delta z}{2})$  is the maximum extent for  $\bar{B}$  overall. All values of  $\bar{B}$  within this range are applicable at radii from

The electron has a  $z$ -equation of motion according to Equation III.3. The functional form for  $\bar{B}$  is then as follows:

$$\bar{B} = \frac{1}{T} \int_0^T -rz \frac{B_0}{L^2} \hat{r} + \left( \left( z^2 - \frac{r^2}{2} \right) \frac{B_0}{L^2} + B_0 \right) \hat{z} dt$$

$$= B_0 \left( 1 + \frac{z_{\max}^2}{2L^2} \right) - \frac{B_0 r^2}{2L^2} \hat{z}. \quad (\text{III.19})$$

## 2. Applying the On-axis Solution Off-axis

The on-axis solution of Section III.A applies to this calculation with the change of variables according to Equations III.15 – 17. This gives the form of Equation III.20.

$r = 0$  through a maximum radius determined by the Heaviside function  $H\left(\frac{B'_0 + B'_{\max}}{2} - \bar{B}\right)$ . The bounds for  $r$  applicable to this range of  $\bar{B}$  are given by

$$0 < r < L \sqrt{2 \left(1 + \frac{(\frac{\Delta z}{2})^2}{2L^2} - \frac{\bar{B}}{B_0}\right)}. \quad (\text{III.23})$$

Thus, integrating Equation III.20 over each of the three subranges of  $\bar{B}$  based on the range of  $r$  applicable to each subrange produces the piecewise probability density function in Equation III.24 at the top of the next page.

$$\begin{aligned}
B'_0(r_{\max}) \leq \bar{B} < B'_0(r=0) &: \frac{2\pi L^3 \bar{B}}{(B_0)^{\frac{3}{2}}} \left[ \frac{1}{\sqrt{\left(2\bar{B} - B_0 + \frac{B_0 r_{\max}^2}{2L^2}\right)}} - \frac{1}{\sqrt{\bar{B}}} \right] \\
B'_0(r=0) \leq \bar{B} < \bar{B}(r_{\max}, \frac{\Delta z}{2}) &: \frac{2\pi L^3 \bar{B}}{(B_0)^{\frac{3}{2}}} \left[ \frac{1}{\sqrt{\left(2\bar{B} - B_0 + \frac{B_0 r_{\max}^2}{2L^2}\right)}} - \frac{1}{\sqrt{2\bar{B} - B_0}} \right] \\
\bar{B}\left(r_{\max}, \frac{\Delta z}{2}\right) \leq \bar{B} \leq \bar{B}\left(r=0, \frac{\Delta z}{2}\right) &: \frac{2\pi L^3 \bar{B}}{(B_0)^{\frac{3}{2}}} \left[ \frac{1}{\sqrt{\left(\bar{B} + \frac{B_0 \left(\frac{\Delta z}{2}\right)^2}{2L^2}\right)}} - \frac{1}{\sqrt{2\bar{B} - B_0}} \right]. \quad (\text{III.24})
\end{aligned}$$

### 3. Comparison to the Monte Carlo

In a Monte Carlo simulation, a series of similar calculations can be performed. Each of some number of electrons is randomly assigned a position  $z$  within the  $z$ -extent of the trap, an initial pitch angle  $\phi$  with respect to the  $z$ -axis, and some radius of orbit  $r$  with respect to the  $z$ -axis. With this information, the simulation calculates the magnetic field experienced by each electron and determines whether it is trapped according to the range of allowable trapping angles.

If an electron is indeed trapped, the simulation will calculate the average magnetic field it experiences, and a histogram of the determined  $\bar{B}$ -values is plotted. Overlaying the analytical function in red with this histogram in blue produces Figure III.4, showing close agreement between analytical solution and simulation. Note here that the depth of the trap has been changed with an  $L$  of 0.316 m.

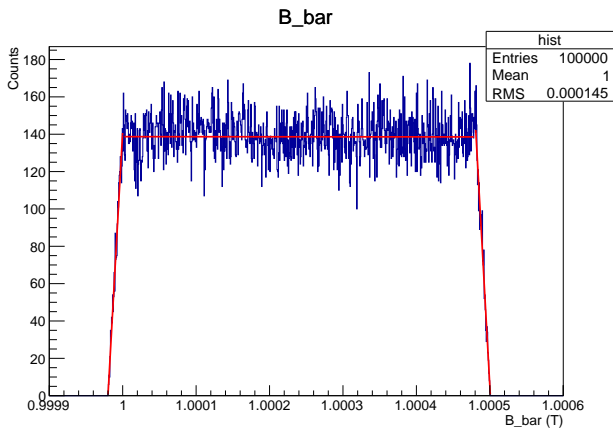


FIG. III.4. Distribution of  $\bar{B}$ -values Off-axis

### C. Efficiency Calculation

As determined in Section III.A.3, decay electrons with pitch angle  $\phi$  within a certain range remain trapped. The fraction of solid angles that remains trapped is a measure of trapping efficiency. With the range of trapped angles from Section III.A.3, the fraction of the solid angles remaining trapped of  $4\pi$  total is as follows:

$$\sqrt{\frac{2 \left( \left( \frac{\Delta z}{2} \right)^2 - z^2 \right)}{2L^2 + 2 \left( \frac{\Delta z}{2} \right)^2 - r^2}}. \quad (\text{III.25})$$

A constant value for  $r$  is assumed. The measure of half the  $z$ -extent of the trap ( $\frac{\Delta z}{2}$ ) is allowed to vary for each of five values of the parameter  $L$ . Thus, integrating III.25 over  $z$  from 0 to  $\frac{\Delta z}{2}$  produces the fractional solid angle trapped as a function of  $\frac{\Delta z}{2}$ ,  $L$ , and the constant  $r$ . This fraction is given by

$$\sqrt{\frac{2}{2L^2 + 2 \left( \frac{\Delta z}{2} \right)^2 - r^2}} \left( \frac{\pi \frac{\Delta z}{2}}{4} \right). \quad (\text{III.26})$$

Similarly, in a Monte Carlo simulation, five values for  $L$  are considered. For each value of  $L$ ,  $\frac{\Delta z}{2}$  takes on the first in a range of 250 values between some pre-established maximum and minimum. The  $z$ -axis is then uniformly populated with electrons within this range of  $z$ , and each electron is uniformly assigned some  $r$  within the established, constant  $r$ -extent and some pitch angle  $\phi$  with respect to the magnetic field. The simulation checks to see whether each electron is trapped and keeps a running tally of the number of electrons generated. This process continues until 250 electrons are trapped. The ratio of the number of electrons trapped (250) to the total number of electrons generated is another way of expressing the trapping efficiency for that particular combination of  $L$ ,  $\frac{\Delta z}{2}$ , and  $r$ . This process continues for each value of  $\frac{\Delta z}{2}$  desired. Then, the entire process repeats for each of the four subsequent values



of  $L$ . This produces Figure III.5, where the value of  $L$  increases from the top trace to the bottom.

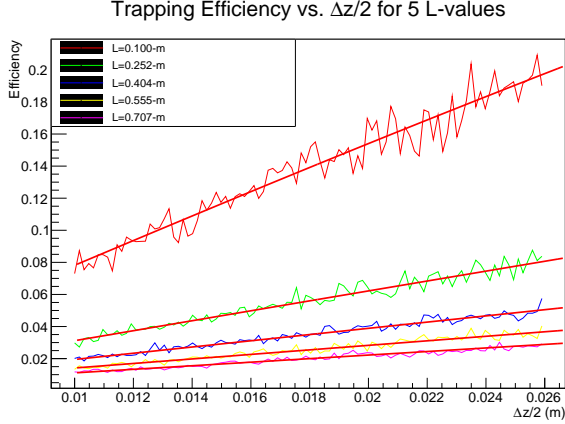


FIG. III.5. Efficiency Measures for 5  $L$ -values and Varying  $\frac{\Delta z}{2}$

This Figure III.5 indicates that trapping efficiency decreases with increased values of  $L$ , which holds true according to Equation III.26. In addition, trapping efficiency increases for each  $L$ -value with  $\frac{\Delta z}{2}$ , which is also evident from Equation III.26.

#### IV. COMPARISON TO ENERGY SPECTRA FROM PROJECT 8

As described in Section II, the magnetic field distributions of Section III can be used to create an energy spectrum for decay electrons. Through manipulation of the Monte Carlo simulation of Section III.B., the steps and results of this process can be conveyed. In the same Monte Carlo simulation, frequency measurements for each trapped electron are obtained by arbitrarily assuming the kinetic energy of each at 30 keV. Then, the angular frequency  $\omega$  for each trapped electron can be approximated to the following:

$$\omega = \frac{e\bar{B}}{\gamma m}, \quad (\text{IV.1})$$

where a substitution of 30 keV is made into the  $\gamma$  term, and  $\bar{B}$  is the average magnetic field the particular electron is calculated to experience. Then, with a frequency measurement for each electron, the  $\gamma$  for each can be evaluated based on the average magnetic field  $\bar{B}$  it is most likely to experience. Since Figure III.4 has a relatively square shape, the likely field selected is 1.002-T. This substitution for  $\bar{B}$  is made into the following:

$$\gamma = \frac{q\bar{B}}{\omega m}, \quad (\text{IV.2})$$

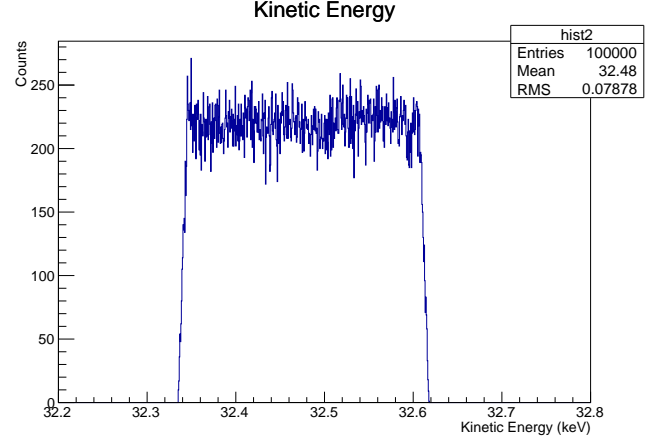


FIG. IV.1. Energy Spectrum Comparison

where  $\omega$  is again the electron's already determined angular frequency. Knowledge of each electron's new  $\gamma$  allows for the calculation of the kinetic energy ( $K$ ) in keV of each, where

$$K = (\gamma - 1) * 511. \quad (\text{IV.3})$$

This produces a spread in kinetic energies that appears as in Figure IV.1. The width of the spectrum in Figure IV.1 is comparable to that of the Project 8 energy spectrum near these values of the kinetic energy[1].

#### V. ACKNOWLEDGMENTS

My sincerest gratitude belongs to REU organizers Dr. Subhadeep Gupta, Dr. Alejandro Garcia, Dr. Shih-Chieh Hsu, and Dr. Gray Rybka for allowing me to work at the Center for Experimental Nuclear Physics and Astrophysics under NSF funding. I am very appreciative of the Helium-6 group for making me feel welcome and comfortable with asking questions from the start of my experience. I am grateful to my advisors, Dr. Alejandro Garcia and Dr. Matt Sternberg, for each has selflessly given their expertise and time to my learning process. Daily, Matt has graciously shared with me both his office and an immense amount of knowledge, the best of gifts I believe one can share.

Three influential men who have presented countless opportunities for me to learn and grow are my professors at W&J: my mentor Dr. Michael McCracken, Dr. Joel Cannon, and Dr. Bill Sheers. These three have collectively played a role in cultivating a passion within me for my work, and I cannot thank them enough for believing in possibilities for my future alongside me.

I would be remiss if I did not acknowledge the role the late Dr. Michael Pettersen has played in



my Physics career as well. In this research and always, I remind myself how lucky I am to have begun

my journey through Physics under the guidance of a truly inspirational man.

---

[1] “Single-Electron Detection and Spectroscopy via Relativistic Cyclotron Radiation.” DOI: 10.1103/PhysRevLett.114.162501.

[2] “UW apparatus measures single electrons radiation to try to weigh a neutrino.” *UW Today*. University of Washington, 2015. Web. April 2015. [www.washington.edu](http://www.washington.edu).